

Polarized Laser Beam Scattering through Turbid Medium for Application in Tissue Imaging

Shamaraz Firdous* and Masroor Ikram

Department of Physics and Applied Mathematics, Pakistan Institute of Engineering and Applied Sciences (PIEAS), Nilore 45650, Islamabad, Pakistan.

* Corresponding author, E-mail: sfirdous@pieas.edu.pk

Received 9 Jul 2004

Accepted 22 Feb 2005

ABSTRACT: We present the experimental results for scattering intensity which arises from illumination of turbid medium with laser light for characterizing the different types of particles. The imaging of tissue like phantom provides the possibility of modeling the laser tissue interaction parameters for the diagnostic of malignant disease and determining the optical properties of a material. Analytical modeling of optical materials with Stokes Mueller matrix provides a unique solution for characterization of sample material. The soybean oil (turbid medium) having properties of interloped phantom is studied. Optics orientation of polarizer-analyzer setup provides the analytical model for turbid medium characterization and can be extended for tissues imaging.

KEYWORDS: optical imaging, soybean oil, Mueller matrix, polarization, turbid medium.

INTRODUCTION

When light, or any electromagnetic wave incidents on a material, it is absorbed, transmitted, reflected, refracted, or scattered. These interactions are defined rigorously via Maxwell's equations. If a medium is comprised of several objects, the fate of the incident wave within the medium is determined by considering the cumulative interactions. If a series of assumptions can be made, these relatively complex equations can be replaced with simpler expressions of geometric optics. Using these equations, one can write an expression for the conservation of the radiative energy along a given direction in the medium. The absorbed energy is promptly converted to thermal energy (heat), and the scattered energy is re-distributed throughout the medium. This scattered energy carries the information about the medium, and if it is quantified properly, it may help characterization of the objects in the medium.¹

Recently, however, there have been a number of experimental and theoretical studies carried out regarding polarized light propagation and scattering in random media for applications in tissue imaging.²⁻⁵ Various experiments have demonstrated that depolarization requires longer length scales than those needed for diffusion. In that case, polarization characteristics of scattered waves provide another and potentially more effective way to discriminate between different kinds of optically thick media. Since change in polarization only occurs from scattering, early-

transmitted responses co-polarized with the incident light have suffered very little scattering. Therefore, examining the polarization state of transmitted responses by scattering media provides a simple and effective way to discriminate between ballistic and snake photons from diffused ones in optically thick media. This intuition has led to a number of imaging and detection techniques.⁶ Many have also examined differences between linear and circular polarized incident light.⁷⁻¹⁰ Except for very small scatterers, experimental evidence clearly suggests that circular polarized light transmitted through a scattering medium made up of spherical scatterers requires significantly more scattering to depolarize than linear polarized light. While this phenomenon is present in a variety of settings, this difference is most pronounced for spherical scatterers that are much larger than the wavelength of the incident light.^{6,12} In contrast, experiments show that linear polarized light depolarizes more slowly than circular polarized light for tissue samples. The backscattered response by polarized light exhibit interesting phenomena and backscattered circular polarized light maintains a significant degree of polarization.¹³⁻¹⁴

In this work the theoretical and experimental results for soybean oil turbid medium using the Stokes Mueller matrix concept are briefly studied. These matrices describe the optical properties and images of the scattering medium.

MATERIALS AND METHODS

Scattering model

The measurement of scattering of light through turbid medium is a very complex phenomenon. The illuminating radiation scatters through turbid sample according to Rayleigh and Mie scattering theories depending on the size of the scatterer. The scattering can be elastic or inelastic. The photons traveling through a random medium may be classified into three types: ballistic components that have not undergone any scattering; snake components that have undergone more than one scattering event; and diffused component that is completely randomized directionally and may be modeled through diffusion equation.

In our experiment, we consider forward transmitted photons for characterization of turbid medium. These photons preserve their polarization after passing through scattering sample. The Mueller matrix polarization component of transmitted photons provides useful information about the medium. The next step is the design of an experimental system to obtain the most information for characterization of particles. However, if polarized light is employed to the turbid medium, more accurate and detailed characterization will be possible. This requires the detection of Stokes parameters as a function of scattering angle, which can be accomplished by using a predetermined set of polarizer and retarder. This approach will allow us to quantify the change in the elasticity of the polarization of the scattered light, which yields information about the particles.

The electro-magnetic wave obeys Maxwell's equations at all points. Since an arbitrarily polarized wave can be represented by the superposition of two orthogonally polarized plane waves as¹⁵

$$E_x(z, t) = E_{0x} \cos(kz - wt) \quad (1)$$

$$E_y(z, t) = E_{0y} \cos(kz - wt + \phi) \quad (2)$$

where E is amplitude and ϕ is the phase difference between the waves in z -direction.

Stokes vectors and Mueller matrix

Polarized light can be completely described using

the 4x1 Stokes vector, as demonstrated in Eq. (3). S_0 is the total detected light intensity which corresponds to the addition of any of the orthogonal component intensities, while S_1 is the linear horizontal and vertical, S_2 is the linear +45° and -45°, and S_3 is the right and left circular polarization states. The mathematical expression for Stokes vectors is given as¹⁵

$$\begin{aligned} S_0 &= \langle E_{0x}^2 + E_{0y}^2 \rangle \\ S_1 &= \langle E_{0x} - E_{0y} \rangle \\ S_2 &= \langle 2E_{0x}E_{0y} \cos \delta \rangle \\ S_3 &= \langle 2E_{0x}E_{0y} \sin \delta \rangle \end{aligned} \quad (3)$$

where δ denotes the differential phase shift between the two orthogonally linearly polarized components of the optical field.

The Mueller matrix is a mathematical representation of the optical polarization properties of a given sample in which the Stokes vector of a probing light source can be combined with the Mueller matrix of the sample to determine the polarization state of the detected output beam. For a given sample, this can be accomplished with a minimum of 16 polarization images, as depicted in Eq. (4). More images may be used, such as 36 or 49 polarization images. Using more than 16 images has inherent benefits. The 16-image derivations in Eq. (4) can be made through Table 1 and are achieved by the simplification of the 49 optical orientations. The Mueller matrix of the sample is obtained as¹⁵

$$[M] = \begin{bmatrix} S_{11} & S_{12} & S_{13} & S_{14} \\ S_{21} & S_{22} & S_{23} & S_{24} \\ S_{31} & S_{32} & S_{33} & S_{34} \\ S_{41} & S_{42} & S_{43} & S_{44} \end{bmatrix} \quad (4)$$

The resultant Stokes vector for material under study is given as¹⁶

$$[S_{out}] = [M][S_{in}] \quad (5)$$

Since biomedical imaging applications include measurements in transmission, and scattering modes, we modeled and tested our system for each of these modalities using Eq. (5), where S_{in} is the input, S_{out}

Table 1. Calculation of the 16-image Mueller matrix from addition and subtraction of the output polarization intensities. The notation is as follows: H for horizontal, V for vertical, P for +45°, M for -45°, R for right circular, and L for left circular.

S_{11} =HH+HV+VH+VV	S_{12} =HH+HV-VH-VV	S_{13} =PH+PV-MH-MV	S_{14} =RH+RV-LH-LV
S_{21} =HH-HV+VH-VV	S_{22} =HH-HV-VH+VV	S_{23} =PH-PV-MH+MV	S_{24} = RH-RV-LH+LV
S_{31} =HP+HM+VP-VM	S_{32} =HP-HM-VP+VM	S_{33} =PP-PM-MP+MM	S_{34} = RP-RM-LP+LM
S_{41} =HR-HL+VR-VL	S_{42} =HR-HL-VR+VL	S_{43} =PR-PL-MR+ML	S_{44} = RR-RL-LR+LL

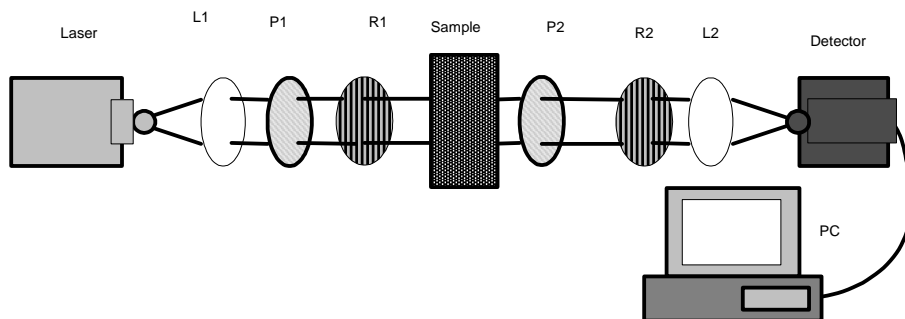


Fig 1. The experimental setup for the measurement of the Mueller matrix elements of the scattering and depolarization effect of turbid sample.

the detected light polarization state and $[M]$ the Mueller matrix for scattering medium.

Experimental Setup

The optical polarimetric imaging system, as shown in Fig. 1, consists of the optics necessary to create the input and output polarization states required for deriving 16 output Mueller matrix of transmitted intensity. The sample is illuminated through He-Ne laser of output power 5 mW at a wavelength of 632.5 nm. The laser beam is focused through lens L1 ($f = 15\text{cm}$) to the polarizer P1 to generate linearly polarized light. The circularly polarized light is generated, by inserting a $\lambda/4$ mica retardation plate R1 behind the linear polarizer, with the retarder principal plane at 45° with respect to the electrical field vector of the incident linearly polarized beam. Light transmitted from sample is then pass through analyzer P2 and retarder R2 and focused by lens L2 on the detector. The turbid sample was prepared from soybean oil having properties like interlaid phantom or polystyrene-sphere suspensions of diameters of 1-7nm.³

RESULTS AND DISCUSSION

In order to detect the fine structural variations of small particles, we have developed the matrix model for characterization of material. We used polarized light produced by unique sets of polarize-retarder to make different and accurate scattering measurements. These unique settings are pre-determined following a series of experiments using the available algorithms. After that, the S_{ij} elements, S_{11} , S_{12} , S_{22} , S_{33} , S_{44} , S_{34} , are recovered from the recorded intensities in a numerical inverse analysis. The output 16 Mueller matrix elements are measured by 49 polarization configurations,¹⁷⁻¹⁸ according to apparatus shown in Fig. 1 and calculation represented in Table 1. The Mueller matrix elements, S_{11} , S_{12} , and S_{34} , indicate the scattering pattern of an object, and if they are determined from experimentally measured scattering signals, they help in characterizing

particle shapes and structures. It is obvious that the angular scattered intensity experiments are not likely to yield much information about the structure of particle as compared to the polarized imaging. The forward scattered and transmitted components are usually difficult to separate. On the other hand, the data of Fig. 2 show clearly that both S_{12} and S_{34} have much more detail, and are more sensitive to the scattering angle. S_{12} can be considered as a measure of depolarization and S_{34} as a change in the polarization of elliptically polarized light. Measurements of these two terms are possible only if we use polarized light and change it systematically. S_{12} and S_{34} are measured by Mueller calculus and describe output linear and circular polarization states of the scatterer. So we can extract both linear and circular images, and examine only these two components. The value of S_{34} in our experimental finding is zero or less than zero and comparable to illuminating wavelength. The element obeys Rayleigh scattering theory and the sample parameters can be extracted through this theory. The output scattered intensity of the sample at different angles through scattering medium is fitted to and the 3rd order polynomial shown in Fig. 2. The output

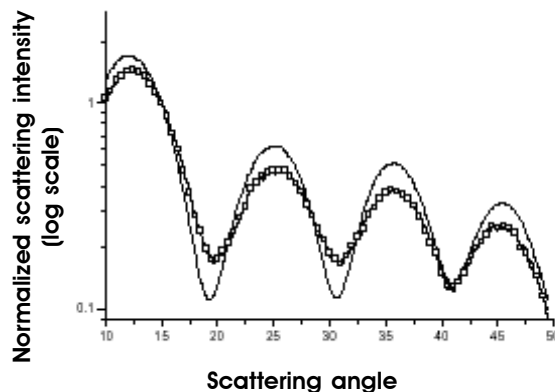


Fig 2. The results of the experimental and fitted intensity of turbid medium. Where the square line represent experimental results and straight line for fitted data.

intensity decreases with increasing scattering angle. The diffused photon scattered larger than ballistic or snake photons.

To explore the possibility of detecting these structural changes, we have constructed several different shapes to determine their scattering signatures using the Mueller matrix calculus.

$$M = \begin{bmatrix} 1.000 & 0.0238 & 0.0398 & 0.0081 \\ 0.0513 & 0.094 & -0.0054 & 0.0701 \\ 0.0059 & -0.0088 & 0.0014 & -0.0130 \\ -0.1015 & -0.0060 & 0.0101 & 0.0103 \end{bmatrix} \quad (6)$$

The phase function information cannot be used alone to identify the particle structures, however, a combined analysis of all three S_{ij} profiles will allow us to determine the required shapes (see Fig. 3). We also note that S_{12} profiles show that sharp-edged particles depolarize radiation more, i.e. S_{12} values for these particles are larger. The Eq. (6) shows all 16 Mueller matrix elements obtained for scattering medium. The particles are smaller in size, which results in a reduced scattering coefficient of 1.9 cm (literature). The displayed intensities are relative to the maximum intensity of the S_{11} element. This element is always positive, however, all other elements can have negative values, because different intensity measurements are subtracted from each other.

The element S_{13} can be obtained by rotating S_{12} by $+45^\circ$. The same relation holds for the pairs S_{31} and S_{21} , and S_{22} and S_{33} . The only difference between the measurements of these pairs is a rotation of the polarization and analyzer optics (P1, P2 in Fig. 1) by 45° . Again, if the material is not optically active and has no preferential optical direction, this result should be expected. Finally, we observe that the elements in the last column, S_{14} , S_{24} , S_{34} and S_{44} , and the last row, S_{41} , S_{42} and S_{43} , are almost zero, while all other elements show strong azimuthal variations in the relative intensity. The differences are the more pronounced azimuthal variation of the center elements, S_{22} , S_{32} , S_{23} and S_{33} . The matrix symmetries are the same as for the phantom. Also, since the reduced scattering coefficients of the two suspensions are identical, the S_{11} elements are the same. The radial intensity decay only depends on scattering and absorption (see Fig. 3). the decline at 5nm depth is due to absorbance of material. This demonstrates the advantages of the Mueller matrix approach over standard video reflectometry, which is based on unpolarized light measurements.

The addition of polarization properties allows distinguishing between the different media. The models, as well as those available from the literature [5], are

likely to provide an extensive database for interpretation of future experimental data. For that reason, we tested the system using polarized light. The detailed results of the experiments are shown in Fig. 4, where the experimental and simulated data for sample is comparable to the Lorenz-Mie theory for spherical particles. The agreement is near perfect for all elements

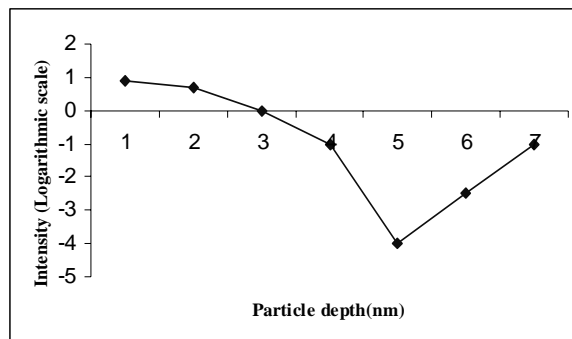


Fig 3. The output intensity with respect to the optical depth of turbid sample.

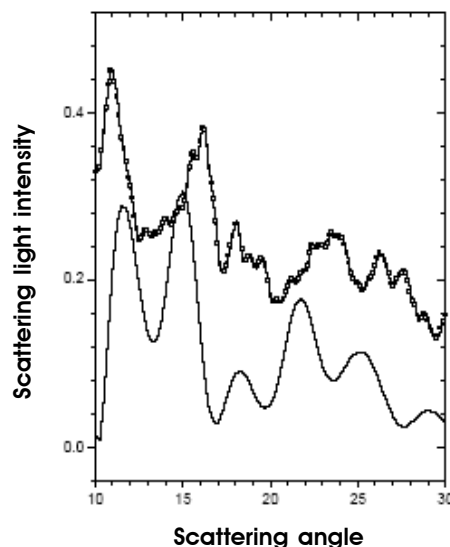


Fig 4. The experimental and fitted data for the normalized output scattered light with respect to the scattering angle of the sample. Where the square line represents experimental results and straight line for fitted data.

of the matrix.

All sixteen Mueller matrix components together provide a "finger print" of the scattering medium under investigation. As just shown, looking at the entire Mueller matrix of Eq.6 often enables one to characterize the media. To obtain a more quantitative distinction between different media, more detailed analyses of single matrix elements are necessary. As an example we investigated changes in the S_{44} element as a function of

particle diameter. The S_{44} element is calculated from four measurements, which involve only circularly polarized light. We found that in the case of turbid sample, S_{44} has no azimuthal dependence. Therefore, we extracted the values of this element along the y-axis from the 2-dimensional images of S_{44} . The results for sample under investigation is shown in Fig. 3. It can be seen that S_{44} decreases with time. Therefore, the suspensions with larger spheres flip the helicity more effectively, and most of the scattered light has a different helicity than the incident light. This behavior can be understood if one considers that with decreasing material depth the sample becomes more and more like a mirror, which can be thought of as a sphere with small radius. If the particles of the medium are small ($d = 1$ nm) compared to the wavelength of 632.5 nm, the scattered light is equally left-hand and right-hand polarized and the element is zero. Furthermore, the effect is strongest in the center, near the laser entry point, where the scattered light has undergone only a few scattering events and the polarization effects are strongest. With increasing sample distance from the point of light incident, the number of scattering events increases and eventually the polarization information decreases. It is obvious that by shape characterization, a material fabrication process can be better understood and improved to achieve the desired structures and size distributions.

SUMMARY AND CONCLUSION

In this paper, we outline the going particle characterization research, and develop an analytical model and material characterization technique for the study of scattered polarized light from highly scattering media. Our method is related to the well-known techniques of Mueller matrix polarimetry. We show that with the use of a polarized incident beam and the analysis of various polarization components in the scattered light, 2-dimensional intensity patterns can be observed. These patterns can be used to gain additional information about the scattering and depolarization. An infinite number of scattering measurements, using polarized light, can be performed by varying the polarization state of the incident beam and detecting different polarization components of the scattered light. However, by introducing the Stokes-vector and the Mueller-matrix concept for scattered light, we provide a framework to select subsets of measurements that comprehensively describe the optical properties of scattering media. With 49 measurements, all 16 elements of the Mueller matrix can be determined. Knowing all 16 elements of this scattering matrix, one can calculate the polarization state of the scattered light given any polarization state of the incident light.

Therefore, by knowing all 16 elements, the medium can be described in terms of optical properties. To illustrate the potential of the Mueller-matrix approach, we studied tissue like turbid sample. The clear differences among different particles can be found in several matrix elements, even when the suspensions have the same scattering and absorption coefficients. We have shown that the S_{44} element, which is obtained from measurements employing right and left-hand polarized light, is especially sensitive to particle sizes in the suspension.

The detailed experimental work is required for Mueller-matrix approach for analyzing scattered light and its potential use in biomedical diagnostics. For example, obtaining the full matrix for particle suspensions with various well-known size distributions may help understanding the patterns observed from biological tissues suspensions. In contrast to suspensions, tissues are highly structured and often have preferred optical axes. These structures should affect the elements of the Mueller matrix. Furthermore, tissues have, in general, a higher scattering coefficient than the suspensions described in this study. Our results provide a basis for imaging tissues and hidden object, which can be used for diagnostic and treatment modalities of malignant diseases. Further investigations are necessary to explore in detail the laser tissue interaction mechanism.

ACKNOWLEDGEMENTS

The authors acknowledge Higher Education Commission Islamabad, Pakistan and appreciate its financial support through "Merit Scholarship Scheme for PhD Studies in Science & Technology".

REFERENCES

1. S. Firdous, M. Ikram, (2004) Characterization of turbid medium through diffusely backscattered polarized light with matrix calculus-I, *IEEE proceeding INCC 2004*, 115-23
2. J. M. Schmitt, A. H. Gandjbakhche, and R. F. Bonner, (1992) Use of polarized light to discriminate short-path photons in a multiply scattering medium, *Appl. Opt.* **31**, 6535-46.
3. A. H. Hielscher, J. R. Mourant, and I. J. Bigio, (1997) Influence of particle size and concentration on the diffuse backscattering of polarized light from tissue phantoms and biological cell suspensions, *Appl. Opt.* **36**, 125-35.
4. S. G. Demos and R. R. Alfano, (1997) Optical polarization imaging, *Appl. Opt.* **36**, 150-55.
5. M. Moscoso, J. B. Keller, and G. C. Papanicolaou, (2000) Depolarization and blurring of optical images by biological tissues, *J. Opt. Soc. Am. A*, **18**, 948-60.
6. E. E. Gorodnichev, A. I. Kuzoviev, and D. B. Gogozkin, (1998) Diffusion of circularly polarized light in a disordered medium with large-scale inhomogeneities, *JETP Lett.* **68**, 22-28.
7. D. Bicout, C. Brosseau, A. S. Martinez, and J. M. Schmitt,

- (1994) Depolarization of multiply scattered waves by spherical diffusers: Influence of the size parameter, *Phys. Rev. E* **49**, 1767-70.
8. V. Sankaran, M. J. Everett, and D. J. Maitland, (1999) Comparison of polarized-light propagation in biological tissue and phantoms, *Opt. Lett.* **24**, 1044-46.
 9. V. Sankaran, J. T. Aonenberger, and D. J. Maitland, (1999) Polarization disc coherently propagating light in turbid media, *Appl. Opt.* **38**, 4252- 61.
 10. E. E. Gorodnichev, A. I. Kuzoviev, and D. B. Gogozkin, (1999) Depolarization of light in small-angle multiple scattering random media, *Laser Physics* **9**, 1210-27.
 11. F. C. MacKintosh, J. X. Zhi, D. J. Pine, and D. A. Weitz, (1989) Polarization memory of multiply scattered light, *Phys. Rev. B* **40**, 9342-45.
 12. S. L. Jacques, J. R. Roman, and K. Lee, (2000) Imaging superficial tissues with polarized light, *Lasers in Surgery and Medicine* **26**,119-29.
 13. G. D. Lewis, D. L. Jordan, and P. J. Roberts, (1999) Backscattering target detection in a turbid medium by polarization discrimination, *Appl. Opt.* **38**, 3937-44.
 14. J. F. de Boer and T. E. Milner, (2002) Review of polarization-sensitive optical coherence tomography and Stokes vector determination, *J. Biomed. Opt.* **7**, 359-71.
 15. L. Jin, T. Hamada, Y. Otani and N.Umeda, (2004) Measurement of characteristics of magnetic fluid by the Mueller matrix imaging polarimeter, *Opt. Eng.* **43**, 181-85.
 16. M. I. Mishchenko, J.W. Hovenier, L.D. Travis, (2000) *Light Scattering by Nonspherical Particles*, Academic Press, New York.
 17. S.Firdous and M.Ikram, (2005) Formulation of Mueller Matrix for Modeling of Depolarization and Scattering of Nitrobenzene in the Kerr Cell, *Appl. Opt.* **44**, 1171-77.